Chapter 5

Effect of modifier concentration on Anticorrosive Properties of Polystyrene-Clay Nanocomposite Coatings on Cold Rolled Steel

5.1. ABSTRACT

A series of polystyrene clay nanocomposite (PSC) coatings containing different concentration of adduct modified clay (AMC) were designed and synthesized to investigate the impact of their chemical structure on the corrosion protection efficiency. PSC coatings with high modifier concentration on Cold rolled steel coupons were found to exhibit better corrosion protection over those of pristine PS based on a series of electrochemical measurements including corrosion potential, polarization resistance, and corrosion current in 3.5 wt % aqueous NaCl electrolyte. The as-synthesized PSC materials were subsequently characterized by FTIR spectroscopy and wide-angle powder X-ray diffraction. From the electrochemical measurements PSC coatings, incorporated with high modifier concentration on cold-rolled steel, were found to be much superior in corrosion protection over the lower concentration. As the concentration was increased there was a significant improvement of properties such as corrosion protection, glass transition temperature and thermal stability of pristine polymer.

5.2. INTRODUCTION

Almost all metals and alloys are unstable in the Earth's atmosphere and will always be subjected to corrosion, i.e., conversion to a lower energy inorganic

compound, such as carbonate, sulfide, or oxide. Thus, the metals and alloys used are in a metastable state and will corrode, at a rate dependent on the environment. Unless steps are taken to minimize the risk of corrosion the result is that corrosion is ubiquitous, taking place in all forms of engineering materials from microelectronics to orthopaedic implants to major civil infrastructures and to the everyday objects in our lives, as illustrated by the collage of images in Figure 5.1 (Hansson., 2011).

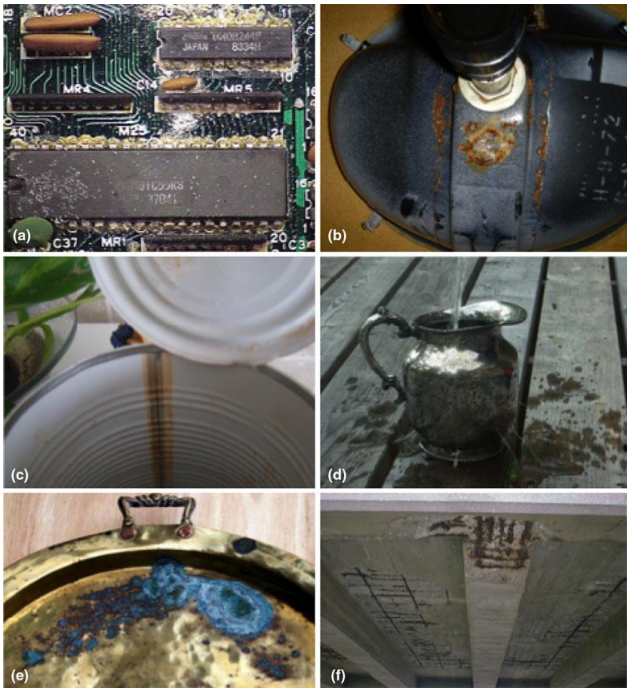

Figure 5.1. Everyday examples of corrosion: (a) corrosion of a computer circuit board (b) crevice corrosion on the underside washroom sink; (c) corrosion of a food can (d) pitting corrosion of a silver-plated water jug (e) corrosion of brass plate and (f) deicing salt-induced corrosion of reinforcing steel corrosion in reinforced concrete bridge.

The most common form of general corrosion is the atmospheric rusting of steel. In this case, the corrosion product is insoluble but is porous and poorly adherent and is, therefore, not protective (Graedel and Frankenthal., 1990). There are many forms of oxides of iron, and rust is often considered to be simply Fe_2O_3.

Recently, clay incorporated polymer composite materials have been extensively studied as protective coating for steel owing to their importance in numerous environmental and industrial applications (Ray et al., 2006; Sanchez, et al., 2005; de Paiva et al., 2008; Bergaya and Lagaly., 2006) Polymer Clay Nanocomposite (PCN) have received great interested over the past decades owing to their light weight coupled with significantly improved physical properties over the unmodified polymer even at low clay concentration(Sánchez-Jiménez et al., 2012; Ratna et al., 2003; Hwang et al., 2009).The improvement in physical properties largely depend on the extend of the dispersion of clay in the polymer matrix. Exfoliation or complete dispersion of clay layers of MMT in to individual clay platelets within the polymer matrix usually leads to largest improvements in physical and chemical properties such as thermal properties (Lan et al., 1994; Giannelis., 1998) mechanical properties (Ratna et al., 2006; Hwang et al., 2009; Kuila and Nandi., 2004), gas barrier properties (Kalendova et al., 2013; Carvalho et al., 2010), flame-retardant properties (Laoutid et al., 2009; Zhu et al., 2002; Wang et al., 2004), and electro-rheology properties (Chang et al., 2007; Chang et al., 2008; Yeh and Chang., 2008).

Recently, it was found that incorporating the inorganic nanolayers of clay into various polymeric matrixes can effectively enhance the corrosion protection effect of pristine polymer (e.g. polyaniline (Shabani-Nooshabadi et al., 2011), polymethylmetacrylate (Zeng and Lee., 2001), polystyrene (Weng et al., 2013), polyimide (Chang et al., 2013) on Cold rolled steel (CRS) based on a series of electrochemical corrosion measurements in saline atmosphere. Montmorillonite (MMT) clay has drawn considerable research attention due to its lamellar display, high inplane strength, stiffness and high aspect ratio. Yeh et.al in 2001, 2002,

2003, 2004, 2005, 2006, 2007, 2008 has reported that the incorporation of organophilic clay platelets into the polymer matrix, in the form of organic based coatings may effectively enhance the corrosion protection of polymer on metallic surface. It's because high level of dispersion of the clay platelets in the matrix polymer effectively increase the length of diffusion path way for O_2 and H^+.

A lot of research has been done on the integration of inorganic nanolayers like MMT clay into the organic polymeric matrices. The findings show that these materials, as a coatings layer, enhance the corrosion protection effect of steel and aluminum in comparison to pristine polymers. These inorganic materials with a plate-like shape are usually employed to effectively increase the length of the diffusion pathways for oxygen and water and decrease the permeability of the coating and lead to corrosion receptivity of coatings (Yu et al., 2004; DeBerry., 1985; Camalet, Lacroix et al., 1996; Meneguzzi et al., 2001)

Several reports have shown the corrosion protection of metals by polymer clay nanocomposite coatings performed at room temperature. Chang et al., 2011 reported the effect of clay for anticorrosion polyaniline coating on metallic surface at high temperature. However, the corrosion protection effect of polystyrene clay nanocomposite coatings using adduct modified clay on CRS has never been reported.

Therefore, in this paper, we present the evaluation of corrosion protection effect of the polystyrene clay nanocomposite materials on CRS in comparison with that of pristine polystyrene by performing a series of electrochemical measurements of corrosion potential, polarization resistance, and corrosion current in 3.5 wt % aqueous NaCl electrolyte. Here we describe a much simpler step for the modification of clay using acid-amine adduct instead of a commonly

used quaternary ammonium salt as intercalating agent and as synthesized PSC materials showed excellent anticorrosive properties. And the effect of modifier concentration on corrosion protection efficiency was studied by varying Acrylic acid-CTAB concentration from 0.5 to 2 meq (milliequivalent) during clay modification. Also the effect of clay loading (1-10 wt.%) were also studied

The PSC materials so obtained were characterized using X-ray diffraction, and infrared spectroscopy. Effect of material composition on the molecular barrier property and thermal stability of a series of PSCs were also studied using electrochemical measurements and Thermogravimetric analysis (TGA), respectively.

5.3. EXPERIMENTAL

5.3.1. Materials

Sodium montmorillonite clay (Na^+-MMT) was obtained from Southern Clay Products, USA with a cation exchange capacity (CEC) of 92.6 meq/100g clay. Styrene monomer (99%), Acrylic acid and Cetyl Trimethyl Ammonium Bromide (CTAB) were purchased from Sigma-Aldrich Chemicals, USA and was used without further purification. The initiator Benzoyl peroxide (BPO) from S.D. Fine Chemical Limited, India was recrystallized from ethanol. Ethanol and methanol was obtained from Merck and were used as received. NMP and Tetrahydrofuran (THF) of HPLC grade was obtained from Merck Specialties Pvt.Ltd., India. Cold rolled steel coupons were used as the coating substrates.

5.3.2. Methods

5.3.2.1. Clay Modification

Adduct modified clay (AMC) were prepared by reacting aqueous Na^+-MMT suspension with calculated amount of equimolar concentration of Cetyl trimethyl ammonium bromide (CTAB) with unsaturated organic acid like Acrylic acid (AA). 1g Na^+-MMT (cation exchange capacity (CEC) = 92 meq/100g) was dispersed in 200 ml distilled water and stirred for 1 h until a homogeneous mixture was formed. Predissolved 2:2 equimolar concentration of the AA- CTAB mixture (equivalent to 2 CEC of the clay) was slowly added to the clay suspension and stirred uninterrupted for 48 h. The resulting AMC was recovered by ultra-centrifuging, washed with ethanol and finally dried at 80°C in a vaccum oven and was designated as AC-AMC2x.

Following the same procedure, modifications were also carried out at different concentrations of modifier like 0.5:0.5(equivalent to 0.5 CEC of the clay), 1:1(equivalent to1 CEC of the clay), 1.5:1.5(equivalent to 1.5 CEC of the clay) and were designated as AC-AMC0.5x, AC-AMC1x and AC-AMC1.5x, respectively. The structure of Acrylic acid-CTAB adduct used for modification was shown below (Figure 5.2).

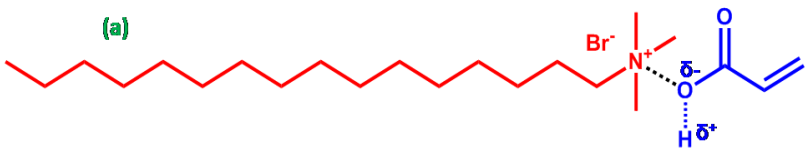

Figure 5.2. Proposed structure of Acrylic acid-CTAB adducts.

5.3.2.2. Synthesis of Polystyrene-clay Nanocomposite

Polystyrene clay nanocomposite was synthesized by in situ intercalative polymerization of styrene using different concentration of Acrylic acid-CTAB adduct. Styrene monomer (1.1 ml) was added to ten percent of the weight of AC-AMC2x. The mixture was ultrasonicated for about 10 min to ensure proper dispersion of the MMT. The flask was degassed with dry nitrogen for about 20 min prior to the addition of 2 wt% BPO initiator. Polymerization was carried out at 70°C by keeping in a temperature controlled oil bath under magnetic stirring (~500 rpm) for 3 h and then at 90°C for 10 h. The solid composite attained was dispersed in minimum amount of toluene, centrifuged to remove insoluble or suspended particles and the soluble fraction was then precipitated in methanol. Finally, the precipitate was filtered and dried under vacuum oven at temperature 60°C to obtain the polystyrene nanocomposite clay (PSC) and was designated as PSC-AC2x.The same procedure were followed for the preparation of PSC using AC-AMC0.5x, AC-AMC1x and AC-AMC1.5x and the composites were labelled as PSC-AC0.5x, PSC-AC1x and PSC-AC1.5x, respectively.

For coating studies, the pristine polystyrene (PS) was synthesized following the same procedure without the addition of AMC. The pristine PS and PSC coating were prepared by dissolving 6 wt.% of the PS and PSC fine powder in NMP solvent. Drops of corresponding solutions were subsequently spread onto the Cold rolled steel (CRS) coupons and cured in an oven at 40°C for 2 h. Then the coated coupons were allowed to completely dry for 24 h at 100°C. The thickness of the coatings was measured by a digimatic micrometer (Mitutoyo) and the film thickness of all the coatings was about 20 ± 2 μm.

5.3.3. Characterization Techniques

The functional group characterization of modified clays was carried out using FT-IR spectroscopy with a fully computerized Nicolet Impact 400D FT-IR spectrophotometer. Samples were mixed thoroughly with potassium bromide and compressed into pellets before recording. All spectra were corrected for the presence of moisture and carbon dioxide in the optical path. The extent of intercalation and exfoliation of AMC and PSC were characterized using WAXS and SAXS, respectively. WAXS and SAXS analysis were conducted on an XEUSS 2D SAXS/WAXS system using a Genix micro source from Xenocs operated at 50KV and 0.3 mA. The Cu-Kα radiation (λ=1.54Å) was collimated with an FOX2D mirror and two pairs of scatter less slits from Xenocs. The d-spacing of the materials were calculated from the angular position 2θ of the observed d_{hkl} reflection peaks based on the Bragg's formula $n\lambda = 2d\sin\theta$, where λ is the wavelength of the X-ray beam and θ is the diffraction angle. Thermal stability measurements were performed at a heating rate of 10°C/min in a nitrogen atmosphere using Shimadzu, DTG-60 equipment.

5.3.3.1. Electrochemical corrosion measurements

The electrochemical measurements of coated samples were carried by using an AutoLab (PGSTAT302N) potentiostat/galvanostat at room temperature. A single compartment conventional three electrode cell setup was used throughout the experiments and the electrolyte was NaCl (3.5 wt.%) aqueous solution. The PS and PSC coating were prepared by dissolving 6 wt.% of the PS and PSC fine powder in NMP solvent. Drops of

corresponding solutions were subsequently spread onto the Cold Rolled Steel (CRS) coupons and cured in an oven at 40°C for 2 h. Then the coated coupons were allowed to completely dry for 24 h at 100°C. The thickness of the coatings measured by digimatic micrometer (Mitutoyo) shows the film thickness of about 20 ± 2 μm. For the electrochemical measurements, coated and uncoated CRS coupons (1 x 1 cm working area) were used as working electrodes, platinum foil was the counter electrode and saturated calomel electrode (SCE) was the reference electrode.

The potentiodynamic polarization and electrochemical impedance measurements were recorded with respect to the open circuit potentials (OCP). In order to get the stable OCP, the cell setup was kept at least 20 minutes prior to start the measurements. In the polarization curves, E_{corr}, I_{corr}, R_p, Tafel slopes, corrosion rates were obtained by the Autolab software. E_{corr} value was obtained by scanning the potential from -500 mV to +500 mV with the scan rate of 5mV/s. In the EIS measurements, R_s, R_p, and R_{ct} values were obtained by Frequency response analyser software (FRS). Frequency range used was 100 KHz to 0.1 Hz. All the electrochemical measurements were replicated at least three times to ensure the reproducibility.

5.4. RESULT AND DISCUSSION

5.4.1. XRD Analysis

Extend of the cation exchange of modified clays were analyzed by WAXD, and the results were plotted in Figure 5.3. It was observed that the (001) diffraction peak of all the AC- AMC appeared at smaller angles (2θ) as compared

to the pristine clay indicating that the cationic exchange took place successfully. The basal space increased from 1.24 nm (2θ = 7.12°) pristine clay to a maximum of 2.12 nm (2θ=4.16°) for AC-AMC2x. Similarly for AC-AMC0.5x, AC-AMC1x and AC-AMC1.5x the basal spacing has increased to 1.45 nm (2θ = 6.1°), 1.86 nm (2θ = 4.74°) and 1.96 nm (2θ = 4.5°), respectively. This result clearly indicate the increase in gallery height of all the AC-AMC was due to the inclusion of Acrylic acid-CTAB adduct within the clay galleries of the unmodified Na^+-MMT during the ion-exchange reaction.

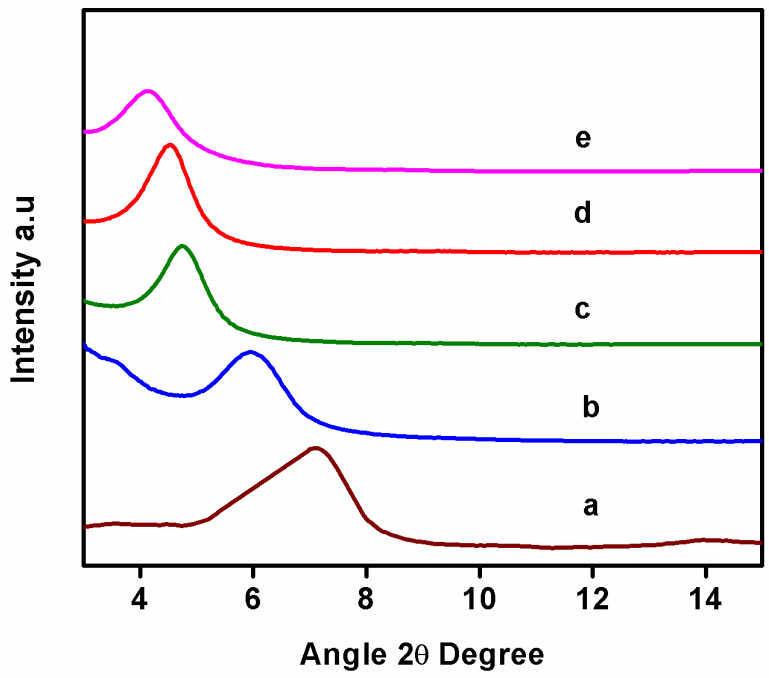

Figure 5.3 X-ray diffraction patterns of (a) pristine clay, (b) AC-AMC2x, (c) AC-AMC1x, (d) AC-AMC1.5x and (e) AC-AMC 0.5x

Figure 5.4A & 5.4B shows the WAXS and SAXS patterns of a series of polystyrene clay nanocomposites with different concentration of modifier. The

d_{001} peak of the clay in all the PSC completely disappeared except for PSC-AC0.5x, indicating the possibility of having exfoliated silicate nanolayers dispersed in the PS matrix (Raju et al., 2016). The vinyl group on Acrylic acid confined within the clay gallery can effectively take part in free-radical polymerization reaction with intercalated styrene molecules (Nair et al., 2010).The absence of the (001) peak suggests that the d_{001} spacing between the layered silicates is intercalated to a spacing greater than the measurable range or clay layers are disorderly dispersed in the polystyrene matrix. The peak at 5.6° (2θ) (17 nm) for PSC-AC0.5x suggests the formation of intercalated polymer nanocomposites. This can be attributed to the finite inclusion of polymer within the inter-gallery of clay, which results in the appearance of a new basal reflection corresponding to the larger gallery height compared to unmodified Na^+ -MMT.

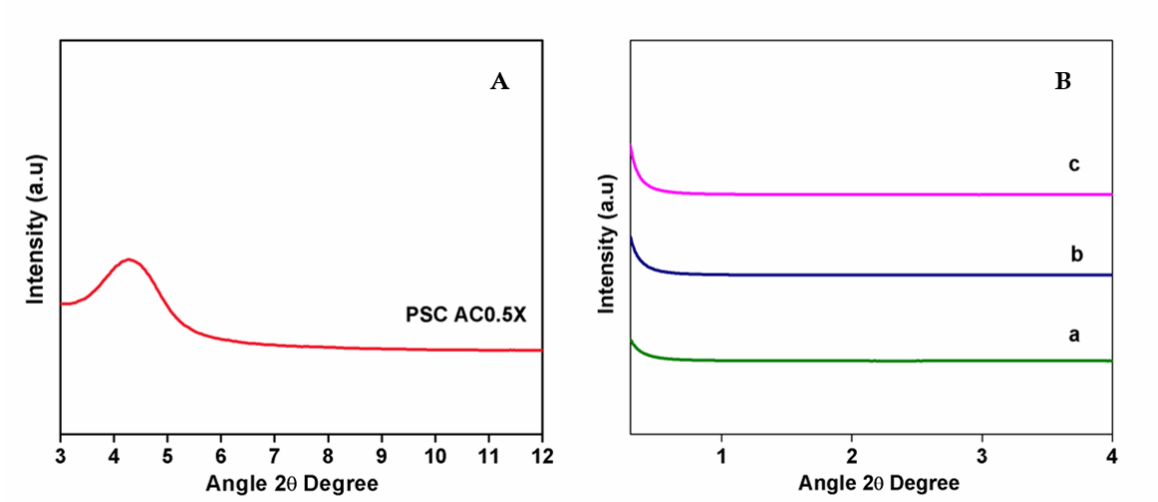

Figure 5.4A. WAXS patterns of PSC-AC0.5x

Figure 5.4B. SAXS patterns of (a) PSC-AC1x, (b) PSC-AC1.5x and (c) PSC-AC2x

From the XRD results it's clear that as the modifier concentration increases, the resulting composite formed is varied from intercalated to exfoliated morphology i.e. d_{001} spacing between the layered silicates is intercalated to a spacing greater than the measurable range or clay layers are disorderly dispersed in the PSC-AC1x, PSC-AC1.5x and PSC-AC2x.

5.4.2. FT-IR Spectroscopy

The successful intercalation of adduct onto the inter-gallery of clay platelets was further confirmed by FT-IR spectroscopy. Figure 5.5 shows the FT-IR spectra obtained for pristine clay and all the four AMC. In all of the FTIR spectra, the characteristic peaks at 1028cm^{-1} and 3445 cm^{-1} are Si-O-Si asymmetric stretching of silicate and structural hydroxyls, respectively. In addition to these two peak for all the three AMC the peaks at 2848 and 2926 cm^{-1} can be assigned to the stretching vibration for $-CH_2$ and $-CH_3$ respectively indicating the presence of long alkyl chain in the modified clay. These bands confirm the intercalation of alkyl group of the CTAB in the interlayer galleries of all the modified clay. Peak at 1642 cm^{-1} is the C=C symmetric stretching frequency of AC-AMC. Peak at 1692 cm^{-1} C=O stretching for conjugated acid of AC-AMC. These two bands confirm the inclusion of acrylic acid group onto the interlayer gallery of clay.

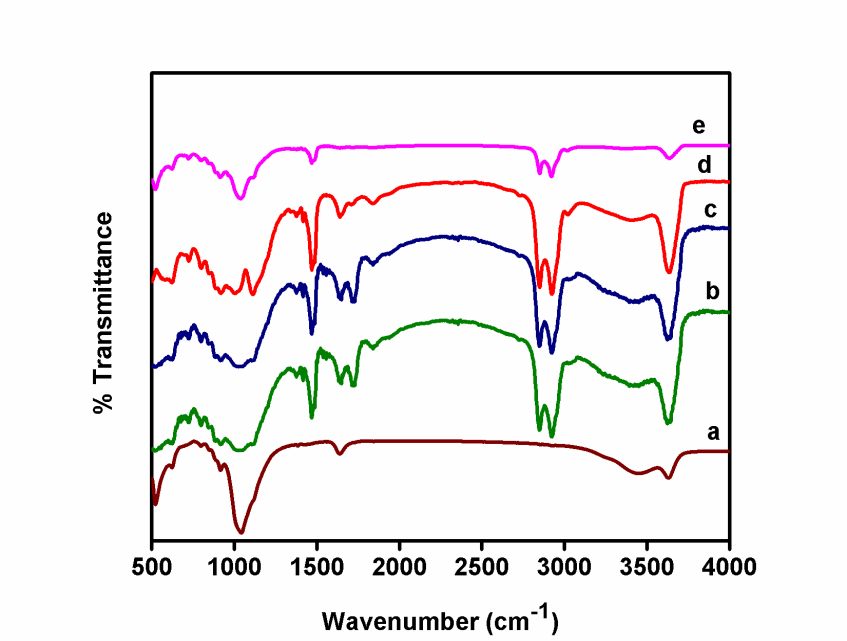

Figure 5.5. FT-IR spectra of (a) Pristine clay, (b) AC-AMC2x, (c) AC-AMC1x, (d) AC-AMC1.5x and (e) AC-AMC 0.5x

From the above FT-IR spectra it's clear that for AC-AMC 0.5x the peak intensity is less compared to other three AMCs. This can be attributed to the presence of low concentration of Acrylic acid-CTAB used for clay modification i.e. 0.5:0.5 (equivalent to 0.5 CEC of the clay).

5.4.3. Potentiodynamic Measurements

In the present study, anticorrosive performance of PSC coated CRS coupons were examined by the values of corrosion potential (E_{corr}), polarization resistance (R_p), corrosion current (I_{corr}) and corrosion rate (R_{corr}). In general, higher E_{corr} and R_p and a lower I_{corr} and R_{corr} indicates enhanced corrosion protection. The Tafel plots for (a) uncoated, (b) PS-coated, (c) PSC-AC0.5x-coated, (d) PSC-AC1x-coated (e) PSC-AC1.5x-coated and (f) PSC-AC2x-coated Cold rolled steel measured in 3.5 wt.% NaCl aqueous solution are shown in Figure 5.6.

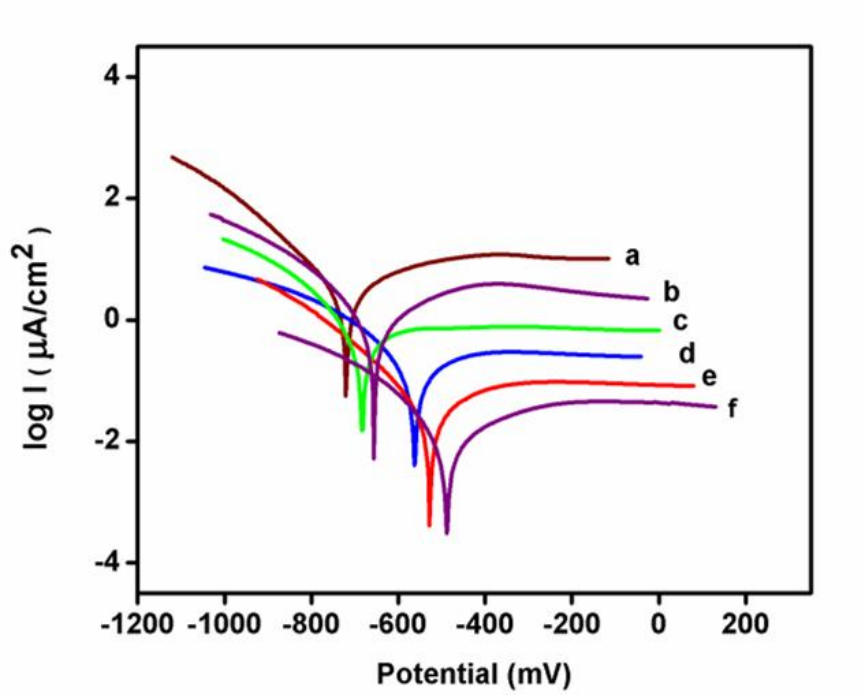

Figure 5.6. Tafel plots for (a) uncoated, (b) PS-coated, (c) PSC-AC0.5x-coated, (d) PSC-AC1x-coated (e) PSC-AC1.5x-coated and (f) PSC-AC2x-coated Cold rolled steel measured in 3.5 wt.% NaCl aqueous solution

Table 5.1.*Electrochemical corrosion measurements of Bare, PS-coated, and PSC-Coated CRS*

SAMPLE	E_{corr} (Mv)	I_{corr} ($\mu A/cm^2$)	R_{ct} ($k\Omega.cm^2$)
Bare	-722	2.4	0.9
PS	-682	1.7	1.8
PSC-AC0.5X	-655	1.07	2.2
PSC-AC1x	-564	0.64	4.7
PSC-AC1.5x	-531	0.51	6.4
PSC-AC2x	-492	0.43	8.2

The results from Figure 5.6 and Table 5.1 indicate that the CRS coupon coated with PS showed a higher E_{corr} (corrosion potential) value than the uncoated CRS. Moreover, it exhibited a lower E_{corr} value than the specimen coated with

PSC materials. For example, the PSC-AC2x-coated CRS showed a high corrosion potential of about -492mV at 30 min. Even after 5 h of measurement, the potential remained at about -500 mV. Such E_{corr} value implies that the PSC-AC-coated CRS coupons are nobler towards the electrochemical corrosion than the neat PS. As modifier concentration increases from 0.5x to 1.5x there is a shift of corrosion potential to positive potential. Moreover, the electrochemical corrosion current (I_{corr}) values of PSC coatings on CRS were found to decrease gradually with increasing modifier concentration. Hence this shows that the better corrosion protection efficiency was observed for the PSC-AC2x composite coating.

This enhanced anticorrosion effect of PS–clay nanocomposite coatings on the metallic surface may be attributed to the barrier effect of MMT clay platelets dispersing in composites. This barrier effect of PSC materials, compared to bulk PS, may be attributed to the dispersing silicate nanolayers of clay in the PS matrix to increase the tortuosity of the diffusion pathway of attacking species like H^+ and O_2 molecules.

5.4.4. Electrochemical Impedance Measurement

Electrochemical impedance spectroscopy (EIS) was used to determine the corrosion activity difference between the surface of uncoated and PS and PSC-coated CRS coupons. Impedance is a complex resistance when a current flow through a circuit made of capacitors, resistors, or insulators, or any combination out of that (Park and Yoo, 2003). EIS measurements result in currents produced over a wide range of frequencies.

For simulation studies, corrosive metals are modelled using an equivalent circuit called a Randles circuit. As shown in Figure 5.7, it consists of a double-layer capacitor connected in parallel with a charge-transfer resistor and in series with an electrolyte solution resistor.Larger the diameter of the semicircle refers to high R_{ct} (charge transfer resistance) value i.e. higher is the corrosion rate.

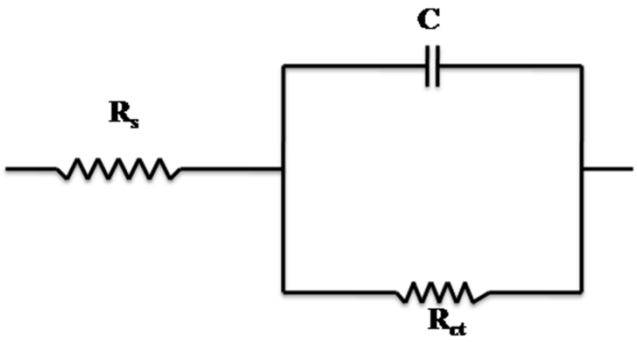

Figure 5.7. Randles circuit

The Nyquist plots measured for six samples of uncoated and coated CRS coupons immersed in 3.5 wt.% NaCl aqueous electrolytes are shown in Figure 5.8. The charge transfer resistances (R_{ct}) of the uncoated, PS-coated, PSC-AC0.5x-coated, PSC-AC1x-coated, PSC-AC1.5x-coated and PSC-AC2x-coated Cold rolled steel were 0.9, 1.8, 2.2, 4.7, 6.4, and 8.2 $k\Omega.cm^2$, respectively. Coatings with high R_{ct} value offer high corrosion protection. Therefore, from the results it's clear that the PSC-AC2x coatings showed higher R_{ct} value and could offer more effective corrosion protection. This novel property of enhanced anticorrosion effect of PSC materials can be attributed to the effective dispersion of clay platelets in the PS matrix,

which in turn increase the tortuosity of the diffusion pathway of attacking species.

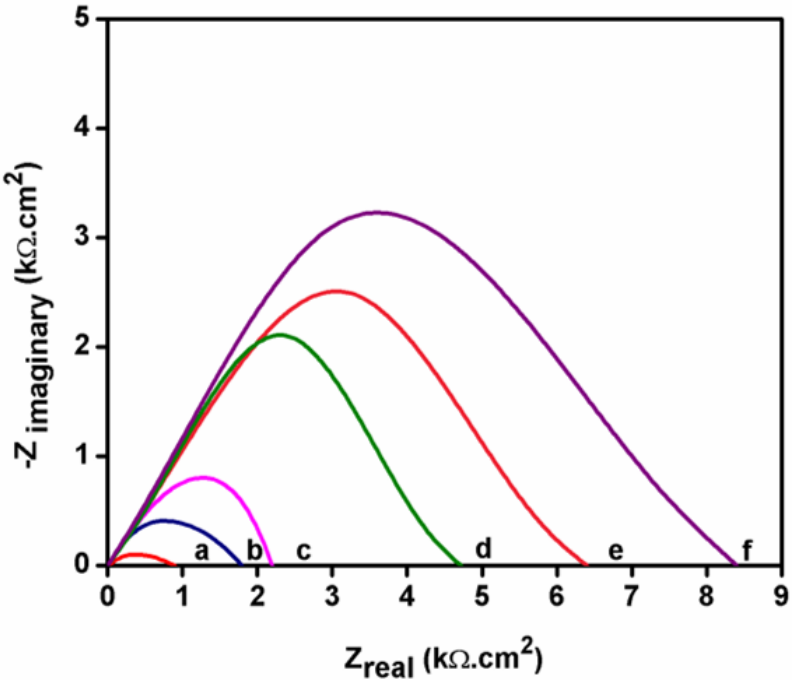

Figure 5.8. Nyquist plots for (a) uncoated, (b) PS-coated, (c) PSC-AC0.5x-coated, (d) PSC-AC1x-coated (e) PSC-AC1.5x-coated and (f) PSC-AC2x-coated Cold rolled steel measured in 3.5 wt.% NaCl aqueous solution.

5.4.5. Thermogravimetric Analysis

TGA has been used extensively to throw light on the precise mode of thermal decomposition. Figure 5.9 shows typical thermogram of weight loss as a function of temperature for PS and the PSC materials up to 600°C. The relative thermal stability of the samples were compared by T_{10} (temperature at 10% mass loss). The temperature T_{10} showed an increase upon increase in modifier concentration (Table 5.2). By the addition of clay, evidently the onset thermal decomposition of all the PSC materials were shifted significantly towards the higher temperature range than that of pristine PS. After 600°C, all curves became

flat and mainly the inorganic residue remained. From the amount of residue at 600°C, the inorganic contents in the original PSC materials can be obtained.

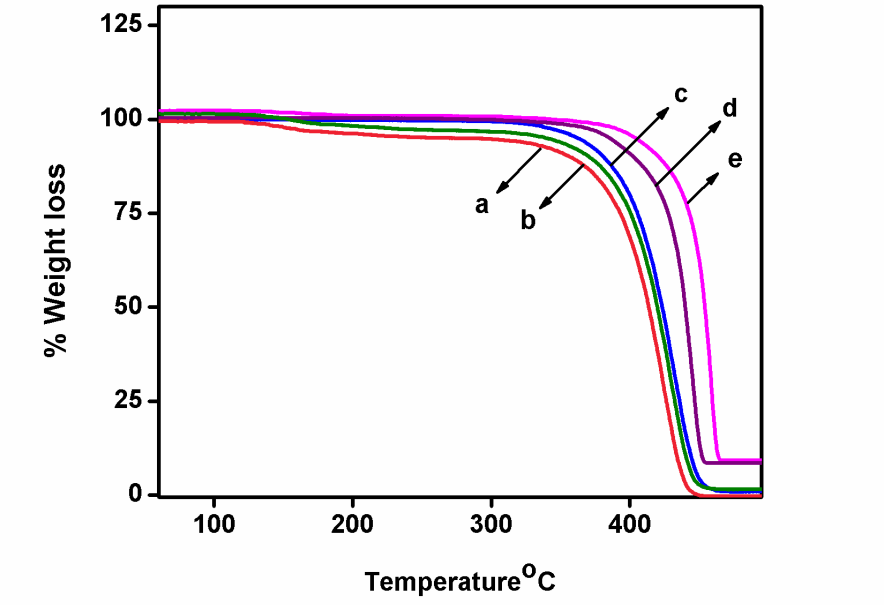

Figure 5.9. TGA curves of (a) PS (b) PSC-AC0.5x (c) PSC-AC1x (d) PSC-AC1.5x and (e) PSC-AC2x

Table 5. 2. Thermal property measurements

Sample	**Thermal Properties**		
	Inorganic content [a] ***(wt.%)***	**T_d** [a] **(°C)**	**T_g** [b] **(°C)**
PS	-	347	76
PSC-AC0.5X	0.5	364	83
PSC-AC1x	2.1	380	100
PSC-AC1.5x	4.0	399	103
PSC-AC2x	7.5	414	109

[a] *As determined by thermogravimetric analysis (TGA).*
[b] *As measured by differential scanning calorimetry (DSC)*

5.4.5. Differential Scanning Calorimetry

The glass transition temperature (T_g) of neat PS and PSC materials were determined by recording DSC scans. Figure 5.10 shows the DSC scan of the entire sample, in which an endothermic shift in the baseline was observed. The T_g of neat PS is at 75°C. Clearly with the increase of the clay content T_g of the nanocomposites increases. This result indicates that the portion of the intercalated PS Chain segments within the silicate galleries tends to retard the segmental motion of the PS matrix and results in a T_g increase.

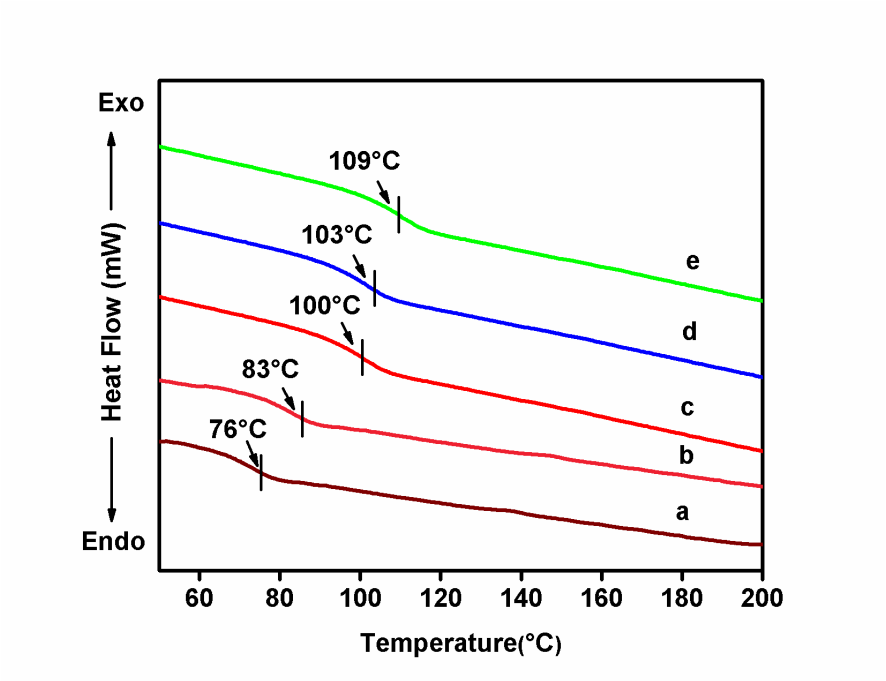

Figure 5.10. DSC curves of (a) PS (b) PSC-AC0.5x. (c) PSC-AC1x (d) PSC-AC1.5x and (e) PSC-AC2x

5.5. Effect of Clay Loading on Corrosion Behavior on CRS

Details of PSC preparation using different clay loading (1, 3, 5 & 10 wt.%) was given in Chapter 4, section 4.3.2 and were designated as PSC-AC1, PAS-AC3, PSC-AC5 and PSC-AC10, respectively. As synthesized PSC materials were

coated on to CRS coupons following the same procedure mentioned in above section 5.3.3.1. Electrochemical measurements were carried out in 3.5 wt.% NaCl and from the tafel plot the PSC-coated CRS electrodes exhibited a higher positive shift in E_{corr} value than that of PS-coated electrode. This positive shift in E_{corr} shows the protection efficiency of PSC-coatings on CRS (Figure 5.11). Moreover, corrosion protection efficiency was significantly improved by increasing the clay loading (i.e., 1-10 wt.%). For example, E_{corr} increased from -492 mV for PSC-AC1 to -625 mV for PSC-AC10-coated CRS (Table 5.3). Therefore, the PSC-AC10 coating with high E_{corr} value -492 mV is more stable and noble towards the electrochemical corrosion.

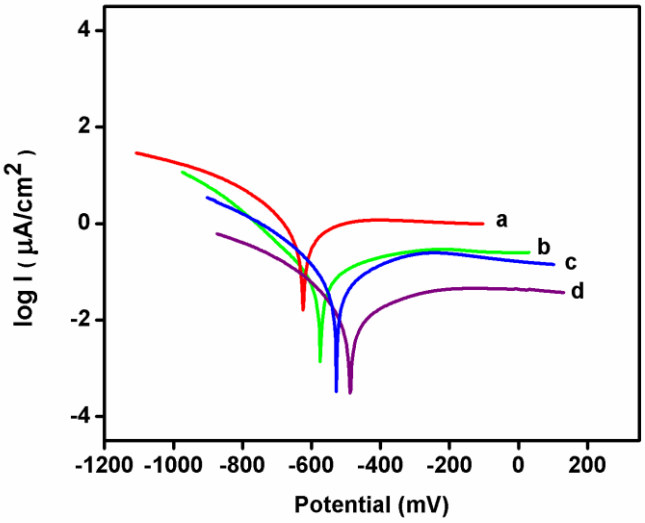

Figure 5.11. Tafel plots for (a) PSC-AC1-coated (b) PSC-AC3-coated, (c) PSC-AC5-coated, and (d) PSC-AC10-coated cold rolled steel measured in 3.5 wt.% NaCl aqueous solution

Table 5.3. Electrochemical corrosion measurements of Bare, PS-coated, and PSC-AC Coated (Different clay loading)

SAMPLE	Feed Composition (wt.%)		E_{corr} (mV)
	PS	MMT	
Bare	-	-	-722
PS	100	-	-682
PSC-AC1	99	1	-625
PSC-AC3	97	3	-576
PSC-AC5x	95	5	-528
PSC-AC10	90	10	-492

5.6. CONCLUSIONS

In summary, a series of PSC materials was prepared by effectively dispersing the organoclay in PS matrix via *in situ* thermal polymerization by varying modifier concentrations on clay. FT-IR and XRD peaks confirmed the inclusion adduct moiety in the intergallery of clay. The PSC materials in the form of coatings on cold rolled steel were found to possess superior anticorrosion performance over those of bulk polystyrene based on a series of electrochemical measurements and impedance spectroscopy in 3.5 wt % aqueous NaCl electrolyte. The corrosion protection efficiency was increased with increase in modifier concentration (i.e. from 0.5x to 2x). PSC coatings with high modifier concentration (PSC-AC2x) on CRS were found to exhibit higher anticorrosion properties. These enhanced corrosion protection efficiency of PSC materials compared to bulk PS result from dispersing silicate nanolayers of clay in the PS matrix to increase the tortuosity of the diffusion pathway of oxygen and water. Similarly, from electrochemical measurement in 3.5 wt % aqueous NaCl

electrolyte it was found that as the PSC coatings with high clay loading (e.g. 10 wt.%) exhibited advanced corrosion protection over those of bulk PS. Also the effects of material composition on thermal stability of PS and PSC materials, in the form of fine powders, were studied by DSC and TGA. However, dispersion of nanolayers of MMT clay in PS-clay nanocomposite materials led to a significant increase in thermal decomposition temperature and also crystalline temperature than that of PS based on the TGA and DSC result. This is tentatively attributed to the confinement of the intercalated polymer chains within the clay galleries that prevents the segmental motions of the polymer chains.